Geochemical Perspectives Letters

Generation of oxidising fluids by comminution of fault rocks

J. Kameda, A. Okamoto

Supplementary Information

The Supplementary Information includes:

- Materials and Methods
- Tables S-1 to S-3
- Figure S-1
- Supplementary Information References

Materials and Methods

Samples

We analysed five natural rock samples collected from an ancient plate subduction boundary (Table S-1): two samples from the Cretaceous accretionary complex in the Shimanto belt, southwestern Japan (shale and oceanic basalt); and three metabasic rock samples from the high-pressure Sanbagawa metamorphic belt, southwestern Japan. The shale and basalt from the Shimanto belt were taken from ancient plate boundary fault rock (tectonic mélange) within the seismogenic subduction zone (Kimura *et al.*, 2012; Kameda *et al.*, 2017). The basic schist samples (basic schist 1, basic schist 2, and basic schist 3) were taken from the chlorite, garnet, and albite–biotite zones, respectively, which correspond to pressure-temperature (*P*-*T*) conditions ranging from greenschist to epidote-amphibolite facies (Enami *et al.*, 1994). The paleo-temperatures of the samples range from ~150 to ~550 °C (Enami *et al.*, 1994). For comparison, quartz sand (Wako Purer Chemicals; grain diameter is ~1 mm) was also used for the experiments. The natural rock samples were gently crushed and sieved to a particle size range of 1.4–8.0 mm before conducting the experiments.

Experimental methods

The grinding experiments were carried out by using a planetary-type ball mill apparatus (P6, Fritsch). An amount of 3 g of each powder was loaded into a zirconia mill pot and was processed at 250–300 rpm for 5 min. The freshly ground 0.2 or 0.3 g powders were then mixed with 10 mL of pure water (Direct-Q 3UV, Merck; pH = 5.84) in a screw-top Teflon beaker, and settled for 10–20 min. The reacted solution was filtered to separate it from solid phases by using a 0.45 μm filter attached to a syringe tip.

The H_2O_2 concentrations of the filtered solutions were measured with the Scopoletin–Horseradish peroxidase (HRP) Fluorometric method using a fluorometer (RF-5300PC, Shimazu) at excitation and emission wavelengths of 380 nm and 460 nm, respectively. Scopoletin (Wako Purer Chemicals) and HRP (Type II, 181 p.u. mg^{-1}; Sigma Aldrich) were used as received. Analytical procedures followed those described by Hurowitz et al. (2007). We also applied the standard addition method with 1 mmol L^{-1} of H_2O_2 spike, whose concentration was adjusted by measuring the H_2O_2 concentration of stock solution by spectrophotometry (V-650, JASCO). The background H_2O_2 concentration of the pure water was determined to be 0.060 μmol L^{-1} by the above method. The measurement error *Sz* for the standard addition method was estimated using the equation described in Larsen *et al.* (1973): $Sz = \pm\frac{Sr}{M}\sqrt{A+B}$, where $A = (n+1)/n$ (n = 3 for this study), $S_r = \pm\sqrt{\sum(Y_0 - \bar{Y})^2/(n-2)}$, $B = (Z-\bar{X})^2/\sum(Z-\bar{X})^2 = D(Y_0-\bar{Y})^2/M^2$, and $Z = -I/M$. $\bar{Y}$ is the mean of the *Y* readings (apparatus response); Y_0 and *I* are the intercepts of the fitted line for three data points to the abscissa and the ordinate axis, respectively, from each analysis; and *M* is the slope of the fitted line.

The specific surface areas of the processed powders were measured using an automated sorption analyser (Autosorb, Quantachrome Instruments). Prior to measurement, the ground powder separated from the solution was dried and degassed at 120 °C for 1 h. Nitrogen adsorption assessed at 77 K provided isotherms for Brunauer–Emmett–Teller (BET) analysis.

Whole-rock major element concentrations and gravimetric loss on ignition (LOI at 950 °C for two hours) were determined by an X-ray fluorescence spectrometer (XRF; Rigaku 25X Primus IV) using the conventional glass bead method at Tohoku University. Wet chemical analyses for determination of the $Fe^{2+}/\Sigma Fe$ ratios were performed by the chemical laboratory of Palynosurvey Co.

The XRD patterns were obtained using a MAC Science MX-Labo with monochromatised Cu Kα radiation at 40 kV and 30 mA, with 1° divergence and antiscattering slits, and a 0.15 mm receiving slit in continuous scan mode at a rate of 1° 2θ min^{-1}. The powders, mixed with an internal standard (corundum, AX-5H,

Hinomoto Kenmazai Co.) at a weight ratio of 4:1, were mounted by side-loading to minimise the development of a preferred alignment of clay minerals. XRD patterns were quantitatively analysed using RockJock software (Eberl, 2003).

Supplementary Tables

Table S-1 H_2O_2 production from surfaces of comminuted samples.

	Qtz1	Qtz2	Basalt	Basalt-a	Shale	Shale-a	Basic schist 1	Basic schist 1-a	Basic schist 2	Basic schist 2-a	Basic schist 2-b	Basic schist 3	Basic schist 3-a
Powder weight (g)	4	4	0.2	0.2	0.3	0.3	0.2	0.2	0.2	0.2	0.2	0.2	0.2
Solution volume (mL)	8	8	10	10	10	10	10	10	10	10	[b]10	10	10
Concentration (μmol L^{-1})	0.08	0.06	0.94	0.72	1.30	0.72	0.48	0.46	0.64	0.72	0.66	0.74	0.51
Specific surface area (m^2 g^{-1})	0.46	0.46	9.01		17.76		6.19		4.47			3.56	
H_2O_2 productivity (nmol m^{-2})	0.55	0.44	5.23	3.99	2.44	1.35	3.86	3.70	7.17	8.04	7.37	10.40	7.51
error	0.046	0.014	0.094	0.179	0.064	0.035	0.193	0.286	0.072	0.181	0.000	0.522	0.229
pH	-	-		10.04		8.71		8.76		9.92	9.72		9.52
[a]Temp. (°C)	-	-	130-190		175-200		300-360		420-500			500-550	

[a] Palaeotemperature data are from Enami *et al.* (1994), Ohmori *et al.* (1997), and Kameda *et al.* (2017).
[b] 0.01 M NaCl solution.

Table S-2 Whole-rock mineral compositions determined using RockJock.

	Basalt	Shale	Basic schist 1	Basic schist 2	Basic schist 3
SiO_2	49.86	59.12	51.15	41.76	42.69
TiO_2	1.63	0.76	1.42	0.89	2.99
Al_2O_3	15.07	18.90	14.45	17.70	13.19
Fe_2O_3	9.45	6.45	12.88	9.74	17.64
[a]FeO	5.50	4.15	6.63	2.73	8.16
MnO	0.19	0.08	0.21	0.15	0.28
MgO	8.46	2.86	6.73	4.03	6.31
CaO	8.51	0.50	8.25	14.94	6.01
Na_2O	3.85	1.23	1.93	1.93	1.72
K_2O	0.75	4.49	0.43	1.61	2.01
P_2O_5	0.15	0.12	0.12	0.11	0.36
LOI	4.37	5.57	3.77	8.11	3.20
Total	102.29	100.08	101.35	100.97	96.40

[a] Data from wet chemical analyses.

Table S-3 Whole-rock chemical compositions.

	Qtz1	Qtz2	[b]Basalt	Shale	Basic schist 1	Basic schist 2	Basic schist 3
Quartz (4)[a]	100.0	100.0	0.0	21.7	10.5	15.0	8.3
Plagioclase (4)	0.0	0.0	45.1	11.4	29.8	21.5	13.0
Chlorite (3)	0.0	0.0	23.9	18.3	37.5	34.0	19.5
Mica (3)	0.0	0.0	0.0	48.6	3.6	0.0	17.7
Amphibole (2.5)	0.0	0.0	0.0	0.0	5.1	13.4	33.9
Epidote (1.66)	0.0	0.0	0.0	0.0	11.5	14.6	5.6
Pyroxene (2)	0.0	0.0	24.1	0.0	0.0	0.0	0.0
Non-silicates	0.0	0.0	6.9	0.0	2.0	1.5	1.9
Total	100.0	100.0	100.0	100.0	100.0	100.0	100.0
Weighted mean of *c*	4.0	4.0	3.0	3.3	3.2	3.1	2.9

[a] Number in parenthesis is the *c* number of each mineral.
[b] Data on mineral composition are from Kameda *et al.* (2017).

Supplementary Figure

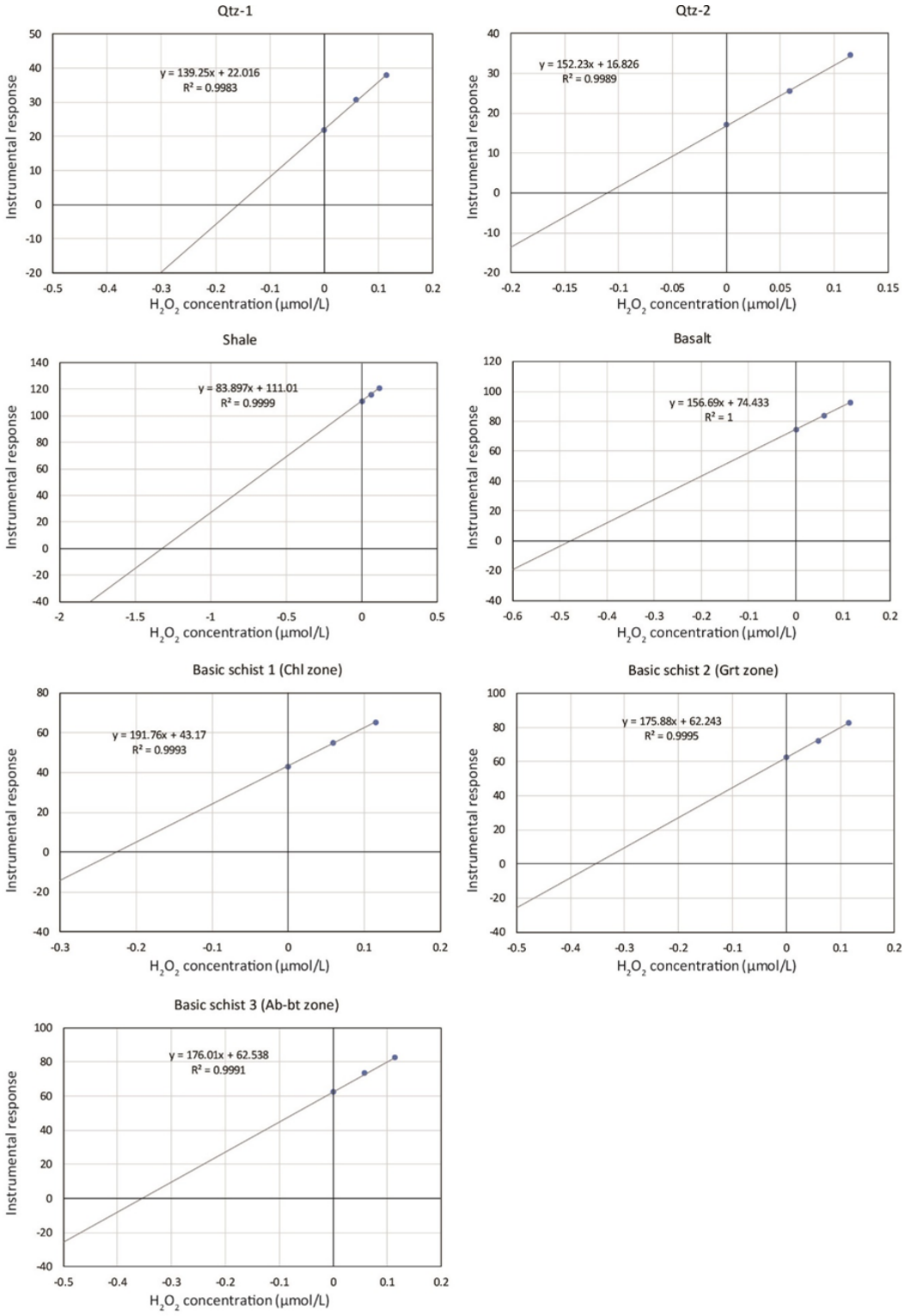

Figure S-1 Results of measurements using the standard addition method. Horizontal and vertical axes are H_2O_2 concentration (μmol L^{-1}) and instrumental response, respectively.

Supplementary Information References

Eberl, D.D. (2003) User's guide to RockJock-A program for determining quantitative mineralogy from powder X-ray diffraction data. *USGS Open-file Report* 03–78.

Enami, M., Wallis, S.R., Banno, Y. (1994) Paragenesis of sodic pyroxene-bearing quartz schists: implications for P‑T history of the Sanbagawa belt. *Contribution to Mineralogy and Petrology* 116, 182–198.

Hurowitz, J.A., Tosca, N.J., McLennan, S.M., Schoonen, M.A.A. (2007) Production of hydrogen peroxide in Martian and lunar soils. *Earth and Planetary Science Letters* 255, 41–52, doi: 10.1016/j.epsl.2006.12.004.

Kameda, J., Inoue, S., Tanikawa, W., Yamaguchi, A., Hamada, Y., Hashimoto, Y., Kimura, G. (2017) Alteration and dehydration of subducting oceanic crust within subduction zones: implications for décollement step-down and plate-boundary seismogenesis. *Earth Planets and Space* 69, 52, doi: 10.1186/s40623-017-0635-1.

Kimura, G., Yamaguchi, A., Hojo, M., Kitamura, Y., Kameda, J., Ujiie, K., Hamada, Y., Hamahashi, M., Hina, S. (2012) Tectonic mélange as fault rock of subduction plate boundary. *Tectonophysics* 568, 25–38, doi: 10.1016/j.tecto.2011.08.025.

Larsen, I.L., Hartmann, N.A., Wagner, J.J. (1973) Estimating precision for the method of standard additions. *Analytical Chemistry* 45, 1511–1513.

Ohmori, K., Taira, A., Tokuyama, H., Sakaguchi, A., Okamura, M., Aihara, A. (1997) Paleothermal structure of the Shimanto accretionary prism, Shikoku, Japan: role of an out-of sequence thrust. *Geology* 25, 327–330, doi: 10.1130/0091-7613(1997)025b0327:PSOTSAN2.3.CO;2.